

Multicenter cross-calibration of I-123
metaiodobenzylguanidine heart-to-mediastinum
ratios to overcome camera-collimator
variations

著者	Nakajima Kenichi, Okuda Koichi, Yoshimura Mana, Matsuo Shinro, Wakabayashi Hiroshi, Imanishi Yasuhiro, Kinuya Seigo
journal or publication title	Journal of Nuclear Cardiology
volume	21
number	5
page range	970-978
year	2014-10-01
URL	http://hdl.handle.net/2297/39687

doi: 10.1007/s12350-014-9943-z.

Multicenter cross-calibration of I-123 metaiodobenzylguanidine heart-to-mediastinum ratios to overcome camera-collimator variations

Kenichi Nakajima, MD,^a Koichi Okuda, PhD,^b Mana Yoshimura, MD,^c Shinro Matsuo, MD,^a Hiroshi Wakabayashi, MD,^a Yasuhiro Imanishi, RT,^d and Seigo Kinuya, MD^a

^a Department of Nuclear Medicine, Kanazawa University Hospital, Kanazawa, Japan

^b Department of Physics, Kanazawa Medical University, Uchinada, Japan

^c Department of Radiology, Tokyo Medical University, Tokyo, Japan

^d Department of Radiology, Suzuka Central General Hospital, Suzuka, Japan

Received Mar 18, 2014; accepted Apr 23, 2014

doi:10.1007/s12350-014-9916-2

Background. The heart-to-mediastinum ratio (HMR) of ¹²³I-metaiodobenzylguanidine (MIBG) showed variations among institutions and needs to be standardized among various scintiscamera-collimator combinations.

Methods. A total of 225 phantom experiments were performed in 84 institutions to calculate cross-calibration coefficients of HMR. Based on phantom studies, a conversion coefficient for each camera-collimator system was created, including low-energy (LE, n = 125) and a medium-energy (ME, n = 100) collimators. An average conversion coefficient from the most common ME group was used to calculate the standard HMR. In clinical MIBG studies (n = 52) from three institutions, HMRs were standardized from both LE- and ME-type collimators and classified into risk groups of <1.60, 1.60-2.19, and ≥2.20.

Results. The average conversion coefficients from the individual camera-collimator condition to the mathematically calculated reference HMR ranged from 0.55 to 0.75 for LE groups and from 0.83 to 0.95 for ME groups. The conversion coefficient of 0.88 was used to unify HMRs from all acquisition conditions. Using the standardized HMR, clinical studies (n = 52) showed good agreement between LE and ME types regarding three risk groups ($\kappa = 0.83$, $P < .0001$, complete agreement in 90%, 42% of the patients reclassified into the same risk group).

Conclusion. By using the reference HMR and conversion coefficients for the system, HMRs with various conditions can be converted to the standard HMRs in a range of normal to low HMRs. (J Nucl Cardiol 2014;21:970-8.)

Key Words: Metaiodobenzylguanidine (MIBG) imaging • standardization • heart-to-mediastinum ratio • calibration phantom • collimator

INTRODUCTION

I-123 metaiodobenzylguanidine (MIBG) has been used in patients with chronic heart failure, ischemic heart disease, and cardiomyopathy. The most widely accepted application, however, is in patients with heart failure.^{1,2} More than 20-year experiences in this field has been accumulated in Japan, and use of MIBG in

See related editorial, pp. 979-983

Reprint requests: Kenichi Nakajima, MD, PhD, Department of Nuclear Medicine, Kanazawa University Hospital, 13-1 Takara-machi, Kanazawa 920-8641, Japan; nakajima@med.kanazawa-u.ac.jp
1071-3581/\$34.00

Copyright © 2014 The Author(s). This article is published with open access at Springerlink.com

prognostic evaluation is described in Japanese Circulation Society's Nuclear Cardiology Guidelines.³ The neurological application of MIBG has also become common, in particular in patients with Lewy-body diseases.^{4,5}

In most of the MIBG studies, the quantification method was essential in differentiating normal and abnormal sympathetic activity, and also high-risk and low-risk groups. The heart-to-mediastinum ratio (HMR) was a simple ratio of the heart and background, and generally good reproducibility has been reported in a single center analysis.^{6,7} When multiple centers are involved in a study, however, there are some preferences for the location of regions of interest (ROIs), which potentially cause variations among institutions and published studies. More importantly, HMR based on the medium-energy (ME) collimator showed higher values than that based on low-energy (LE) collimators.⁸ The nomenclature of collimators is classified into two major groups of LE and ME, but the camera vendors have created various types of collimators depending on the purpose in order to achieve good balance among resolution, sensitivity, and applicable energy range. The low-medium energy (LME) collimator is one of the examples created to cover the higher energy scatter portion of the ¹²³I energy spectrum, in accordance with the widely used ¹²³I-labeled radiopharmaceutical in Japan.

We have already made a phantom for MIBG planar imaging to cross-calibrate two acquisition conditions.⁹ As an extension of this idea, the purposes of this study were to accumulate MIBG data for the HMR from common vendors, and to establish the cross-calibration method among various camera and collimator combinations. Our hypothesis in this study is that all camera-collimator combinations can be unified to a standard HMR, so that comparison among multiple centers and the previous studies can be practically performed. The validity was also tested in clinical studies.

METHODS

Phantom Design

Details of the phantom were written elsewhere.⁹ In brief terms, since the purpose of this phantom was to standardize the HMR among different collimator types by minimizing effects of septal penetration and Compton scatter, we tried to simplify the structure as much as possible, in order to calculate the same HMR using planar images (Taisei Medical, Co. Ltd, Osaka, Japan; Hokuriku Yuuki, Co. Ltd, Kanazawa, Japan). Each organ part, namely, heart, mediastinum, lung, and liver, was designed so that the radioactivity was distributed uniformly in the organ regions. The size of the phantom was 380 mm in width and length, and each organ was flat with a constant

concentration. The thickness of each organ was adjusted by changing the number of acrylic slices. The acrylic slices, 5 mm in thickness, were pasted with various numbers and orders. The upper and lower slices were 10 mm in thickness. Four HMRs from anterior and posterior views were obtained from two types of the phantom.

A Phantom Experiment

¹²³I-MIBG of 111 MBq in 4,450 mL was prepared and filled into the two phantoms. Since all organ parts were connected as one compartment, no adjustment of radionuclide concentration for each organ part was required. A 3-cm acrylic plate was placed over the phantom when imaging was performed. The 256 matrix images were acquired from the anterior and posterior views for 3–10 minutes, which was a situation comparable to clinical MIBG imaging. The energy was centered at 159 keV with a 20% window. Hospitals using a 15% window also measured HMRs with this condition. The experiments were performed using 225 conditions in 84 institutions (see “Appendix”).

A Mathematical Reference Value of HMRs

HMRs were mathematically calculated in these models, assuming the linear attenuation coefficient (μ) of ¹²³I for water as 0.147 cm^{-1} . The standard equation for attenuation, that is exponential of $(-\mu x)$, where x was thickness of attenuation, was used. For calculation purpose, slices were divided into 0.05 mm slices, and the summation of the count was calculated using Mathematica software (version 9, Wolfram Research, Inc., Champaign, IL). The mathematical reference HMR was the attenuation corrected HMR, while Compton scatter and septal penetration of gamma rays were not included. The reference HMR was 3.50 and 2.60 for the type 1 phantom, and 1.80 and 1.55 for the type 2 phantoms.⁹

Cross Calibrations

A calibration method from LE-type collimator to ME-type collimator comparable values was already described.¹⁰ In this study, 4 or 2 HMRs from 2 phantom types (anterior and posterior views for each) were plotted to the reference values (Figure 1). A linear regression equation was calculated using the formula of $y - 1 = K * (x - 1)$ (* denotes multiplication), in which the line always passes on the coordinate (1,1). The first step was to convert the HMR with LE-collimator to the reference value (HMR_{ref}) using coefficient K_a , which is the slope of the regression line in condition A. The second step was to convert from the HMR_{ref} to a standardized HMR ($\text{HMR}_{\text{standard}}$) using the K_{standard} . The K_{standard} was defined as average K values for typical ME collimators. The conversion coefficient of HMR from LE to the standardized condition was identical to K_{standard}/K_a . The rationale for this conversion to the common ME-type is based on practical consideration, so that most of the users of the ME-collimator can use their routine HMRs.

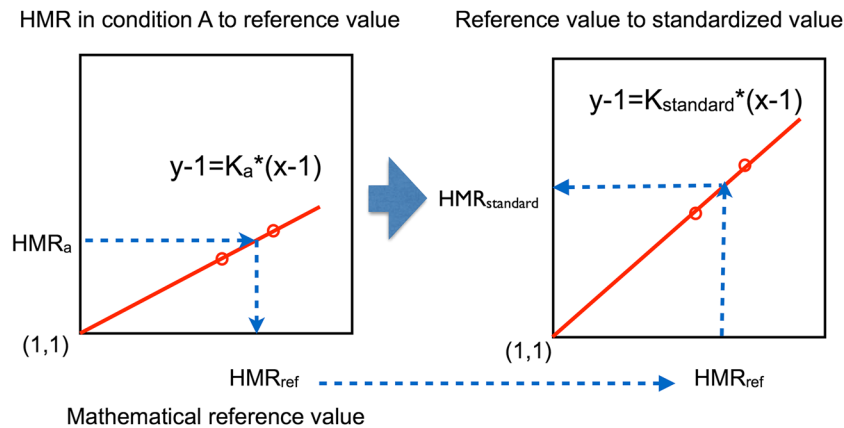


Figure 1. Conversion of HMR from the condition A (HMR_a) to the reference value (HMR_{ref}), and to the standard value ($HMR_{standard}$). In this study, $K_{standard}$ of 0.88 is used as the conversion coefficient, which is an average coefficient of common ME collimators. Asterisk denotes multiplication.

Clinical MIBG Imaging

Anterior MIBG images were obtained with a 256×256 matrix format for 3-5 minutes. In Hospital A, Prism 2000 with a LEHR collimator (Picker, Co. Ltd., Tokyo, Japan) and E.CAM Signature with LMEGP collimators (Siemens Japan Co. Ltd., Tokyo) were used ($n = 12$). In Hospitals B, GCA-9300A three-detector gamma cameras with LEHR (Toshiba, Tochigi, Japan) and LMEGP collimators (Siemens Japan Co. Ltd., Tokyo, Japan) were used ($n = 10$). In Hospital C, E.CAM systems with LEHR and LMEGP (Toshiba, Tochigi, Japan) were used ($n = 15$). In the Hospitals A and B, acquisition energy was set 159 keV with a 20% window, and with a 15% window in Hospital C according to institutional routine conditions. We did not change their preference for routine acquisition conditions. In Hospitals A and B, only a delayed image at 3 hours was obtained with two LE and ME conditions, and in Hospital C both 20-minute (early) and 3-hour (delayed) images were obtained. Thus, a total of 52 studies were obtained by both LE- and ME-type conditions in 37 patients (16 males and 21 females, aged 71 ± 10 years). Indication of the MIBG study was not specified in this technological validation study. However, the indications included ischemic and non-ischemic cardiac diseases suspicious of having heart failure and neurological diseases as Parkinson disease or syndrome, Alzheimer disease, and dementia with Lewy bodies.

HMRs were calculated using a semiautomatic ROI setting software.¹¹ In the software algorithm, the heart region was set as a circle after manually pointing to the center of the heart, and a rectangular region was determined in the upper mediastinum, in which the width was 10% of the body, and the height was the upper 30% of the mediastinum. All the data were anonymized and processed in each hospital, and the calculated data were sent to Kanazawa University. Informed consent was obtained from all patients in each hospital. Ethical committees or comparable institutional regulation approved the study.

Statistics

The data are shown as mean \pm standard deviation. A difference among groups was examined by one-way analysis of variance and Student's t test. The linear regression equation of the HMRs between two conditions was calculated by the least square method. When the HMRs were classified into three risk groups, considering that the average HMR in the normal databases was 2.8 and the lower limit was 2.2, thresholds of ≥ 2.20 (normal range or higher) and 1.60-2.19 (low risk) and < 1.60 (high risk) were used. These thresholds were generally in agreement with the risk classifications used in heart failure patients.^{1-3,12,13} Contingency table analysis was performed and degree of agreement was tested. P values < 0.05 were considered significant. The statistics software JMP version 10 (SAS Institute Inc., Cary, NC, USA) was used, and mathematical calculation was based on Mathematica 9 (Wolfram Research Inc., Champaign, IL, USA).

RESULTS

Number of Experiments and Participating Institutions

A total of 225 experiments were performed in 84 institutions, including 7 camera vendors of Siemens ($n = 71$), GE ($n = 56$), Toshiba ($n = 50$), Shimadzu ($n = 23$), Philips ($n = 19$), Hitachi/Philips ($n = 5$), and ADAC ($n = 1$). Collimator types were divided into two major groups of LE ($n = 125$) and ME ($n = 100$). The LE groups included high-resolution (LEHR), general-purpose (LEGP), all-purpose (LEAP), general-all-purpose (LEGAP), extended LE general-purpose (ELEGP), and cardiac high-resolution (CHR). The ME group included low-medium-energy general-purpose (LMEGP), general-purpose (MEGP), general-all-purpose (MEGAP), low

penetration (MELP), and high-energy general-purpose (HEGP). The nomenclature of collimators depended on manufacturers' specifications.

HMRs Measured in Four Phantom Conditions

When HMRs were obtained using four phantom conditions, the LE-collimator group showed lower values compared with the ME-collimator group. For the phantom of HMR 1.55, LE-collimator (n = 125) and ME-collimator (n = 100) groups showed 1.40 ± 0.06 and 1.51 ± 0.06 ($P < .0001$). Similarly, the phantoms of HMR 1.80, 2.60, and 3.50 showed 1.53 ± 0.07 and 1.69 ± 0.07 ($P < .0001$), 2.00 ± 0.13 and 2.45 ± 0.12 ($P < .0001$), and 2.43 ± 0.19 and 3.10 ± 0.17 ($P < .0001$), for LE and ME groups, respectively. Distribution of the mathematical HMR of 1.8, 2.6 is shown as examples (Figure 2). While both LE and ME groups differed significantly, overlap of histogram distributions was also observed.

Conversion Coefficients Determined by 4 and 2 Data Points

When cross-calibration equations passing on the (x, y) coordinate of (1,1) were made based on all 4 points and higher 2 points, the distribution of coefficients showed high correlation between two methods: (slope from the 2

points) = $-0.0197 + 1.027 \times$ (slope from the 4 points) ($R^2 = 0.997$, $P < .0001$). We therefore used coefficients from the upper two points in the following analyses.

The conversion coefficients to the reference value are summarized according to the main collimator names, namely 5 LE subgroups and 3 ME subgroups (Table 1). Since the ELEGP collimator showed two separate distributions between old (2002-2004) and new (2008-2013) types due to modification of specification, it was divided into two subgroups. The average conversion coefficients were 0.55 for LEHR, 0.65 for LEGP/AP, 0.83 for LMEGP, and 0.88 for MEGP, and the highest was 0.95 for MELP/HEGP types. The difference among subgroups was highly significant (F ratio 214, $P < .0001$). When the conversion coefficient was divided into two groups, the average values were 0.595 ± 0.078 for the LE group and 0.865 ± 0.067 for the ME groups (F ratio 750, $P < .0001$) (Figure 3).

HMRs from LE and ME Collimators and Effect of Standardization

As shown in Figure 4B, D, HMRs from LE-collimator types were corrected using an experimentally determined conversion coefficient to the reference value based on the results of individual hospitals. It was converted again from the reference value to $HMR_{standard}$ using a coefficient of $K_{standard} = 0.88$, which derived from the average coefficient of the MEGP collimator (Table 1). HMRs from ME-collimator types were similarly converted to the $HMR_{standard}$ using $K_{standard} = 0.88$.

HMRs with the LE-collimator group showed significant underestimation; (HMR with LE-collimator) = $0.62 + 0.47 \times$ (HMR with ME-collimator) (Figure 4A). After the correction to standardized HMRs for both LE and ME collimators, they showed comparable values below 2.5. However, underestimation of approximately 10% was observed in an HMR range of >2.5 . The relationship below $HMR < 2.8$ with ME-collimator is plotted in Figure 4C, D.

When the HMR was divided into three groups using the threshold of 2.2 and 1.6, the contingency table showed that the degree of agreement was κ 0.07 (95% confidence of interval [CI] -0.026 to 0.17 , $P = .21$) and complete agreement was 25/52 (48%) between the HMRs from LE and ME types (Table 2). However, the standardized HMR to the average ME-type showed good agreement between the corrected LE-type and corrected ME types (κ 0.83, 95% CI 0.69-0.97, $P < .0001$) and complete agreement was 47/52 = 90%. A total of 22 patients (42%) were reclassified into the same risk groups after standardization.

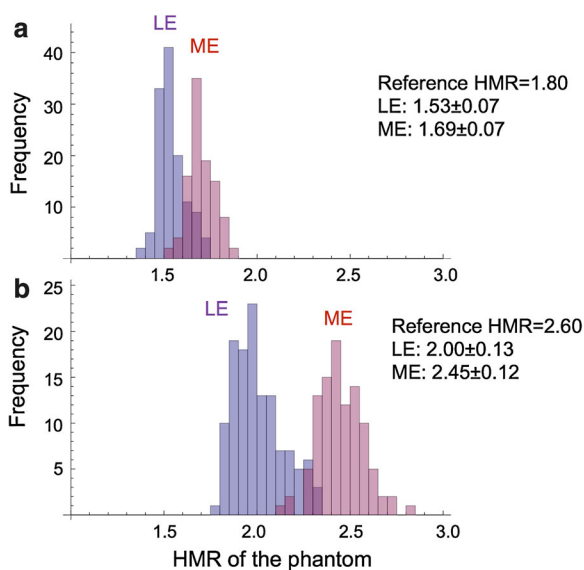


Figure 2. Distribution histograms of HMRs using phantoms with the reference HMR of 1.80 (a) and 2.60 (b). While the ME group shows higher values than the LE group, overlaps are observed.

Table 1. Conversion coefficients to mathematical reference values

Collimator	LE or ME	N	Mean	SD	Lower 95%	Upper 95%	Vendor and number
LEHR	LE	73	0.55	0.05	0.54	0.56	GE (15), Siemens (25), Toshiba (22), Shimadzu (8), Philips/Hitachi (3)
CHR	LE	9	0.55	0.02	0.53	0.57	Philips/Hitachi (9)
LEGP/AP	LE	25	0.65	0.04	0.63	0.66	GE (10), Siemens (3), Shimadzu (7), Philips/Hitachi (4), ADAC (1)
ELEGP (old)	LE	4	0.62	0.03	0.57	0.67	GE (4)
ELEGP (new)	LE	14	0.75	0.03	0.73	0.76	GE (14)
LMEGP	ME	46	0.83	0.05	0.81	0.85	Siemens (25), Toshiba (21)
MEGP/GAP	ME	40	0.88	0.05	0.86	0.89	GE (13), Siemens (9), Toshiba (3), Shimadzu (8), Philips/Hitachi (7)
MELP/HEGP	ME	14	0.95	0.04	0.92	0.98	Siemens (9), Toshiba (4), Hitachi (1)

LE, Low-energy; ME, medium-energy; CHR, cardiac HR; GP, general-purpose; AP, all-purpose; GAP, general-all-purpose; ELE, extended LE; LME, low-medium energy; LP, low penetration; HEGP, high-energy general-purpose.

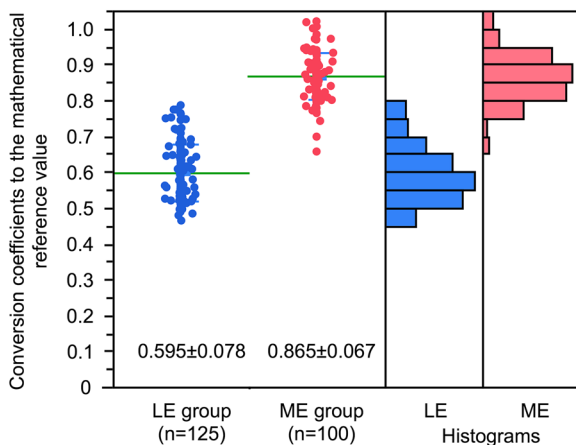


Figure 3. Conversion coefficients to the reference values in LE- and ME-collimator groups. Bars denote average values, and histogram distributions are also shown. Although a significant difference was observed between the mean values of LE and ME groups, an overlap was also noted.

DISCUSSION

As a number of MIBG studies have been performed using the HMR in fields of cardiology and neurology, this study focused on unifying the methods for calculating HMR. Using the calibration phantom experiments and measured conversion coefficients specific for individual camera-collimator systems, all the HMRs could be converted to standardized HMRs using the average conversion coefficient of the commonest ME types. The standardized HMRs were applicable to multiple institutions in the range of normal to low HMR values.

The difference in collimator types is one of the most important factors that affect the variation of HMRs. In

particular, HMRs derived from ME-type collimators are significantly higher than those from LE-type collimators.^{9,14,15} As shown in the JSNM-working group normal databases of ¹²³I-MIBG, average late HMR was 2.5 and 3.0 for LE-collimator and ME-collimator groups.¹⁶ The EANM Cardiovascular Committee and the European Council of Nuclear Cardiology recommended the use of the ME-collimator, which provided stable results.⁸ However, the classification into two collimator types seems to be too simple today. Collimator specifications have been modified to cover a higher energy of 159 keV of ¹²³I, and the LME collimator, which is widely used in Japan, and extended low-energy collimators have become available. Even in ME types, the effects of septal penetration and Compton scatter depend on the three-dimensional structure of the collimator septa and holes. Therefore, a correction method to integrate a large variation of collimator design was sought after.

Regarding acquisition conditions, both energy windows of 20% and 15% have been used and acquisition time ranged from 3 to 10 minutes in Japan. However, in this study, although we decided on common data acquisition protocol in the phantom study, we did not compel all hospitals to use specific acquisition conditions for clinical MIBG imaging. A minor difference in conversion coefficients might have therefore been observed even with the same collimator due to acquisition conditions. Even with a single vendor's camera and collimator combination, an SD of coefficient was 0.02-0.03 as shown in Table 1. The reasons for this variation might be explained by composite factors such as an energy window (15% or 20%), acquisition time, and back scatter from the opposite detector, SPECT couch and floor. Although fraction of the high-energy

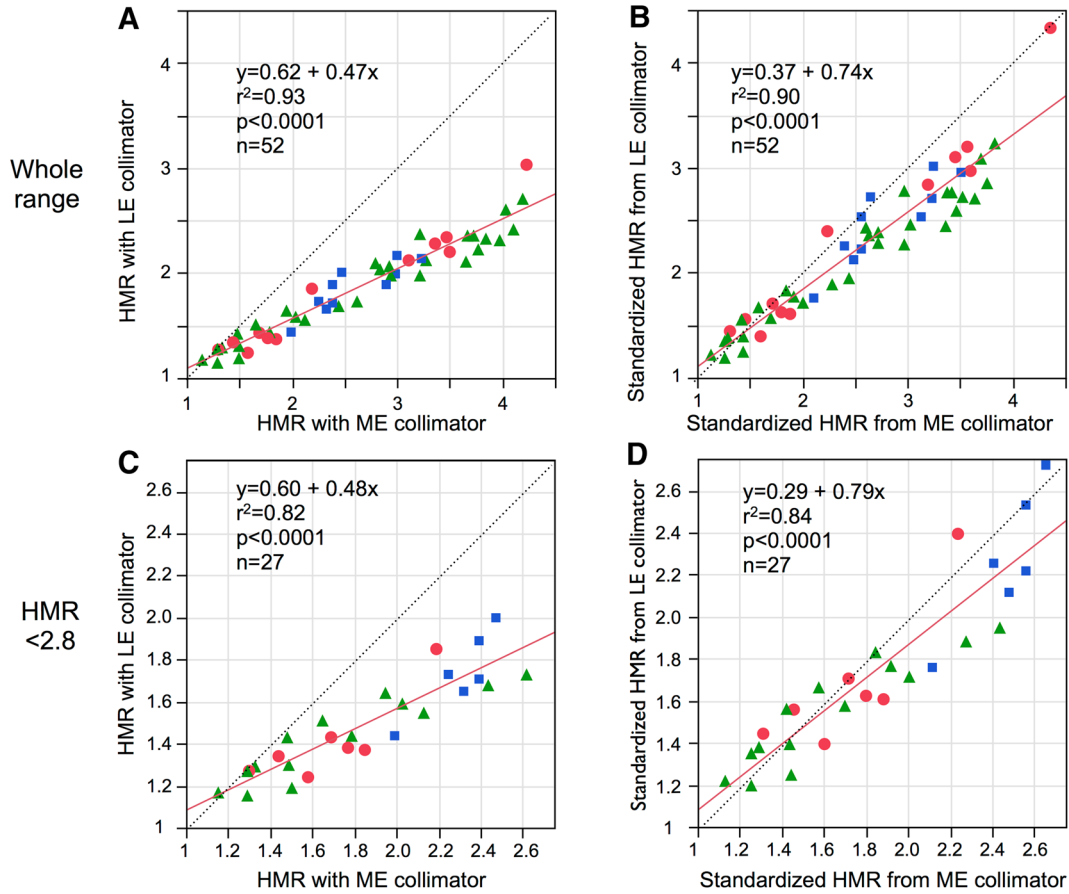


Figure 4. Linear regression lines of HMRs between ME- and LE- collimator types in clinical validation studies. (A, B) show the relationship before and after standardization. (C, D) show the range of HMR <2.8. The marks of circle, square, and triangle are HMRs from three hospitals. Dotted lines indicate line of identity.

Table 2. Contingency table for three HMR risk groups

LE: ME	High risk (<1.60)	Low risk (1.60-2.19)	Normal (≥2.20)	Total
A. HMRs measured with ME- vs LE-collimator types				
High risk (<1.60)	10	0	0	10
Low risk (1.60-2.19)	8	2	0	10
Normal (≥2.20)	0	19	13	32
Total	18	21	13	52
B. Standardized HMR converted from ME- and LE-collimator types				
High risk (<1.60)	10	1	0	11
Low risk (1.60-2.19)	1	7	0	8
Normal (≥2.20)	0	3	30	33
Total	11	11	30	52

A. Degree of agreement: $\kappa = 0.07$, $P = .21$, complete agreement = 25/52 (48%). B. Degree of agreement: $\kappa = 0.83$, $P < .0001$, complete agreement = 47/52 (90%).

photon (529 keV) of ^{123}I is only 1.4%, the effect of down scatter is complicated and troublesome.

While various methods have been proposed to improve the quantification of ^{123}I tracers, including a multiple energy window method,^{9,15} deconvolution of the septal penetration method,¹⁷ and a direct empirical conversion method,¹⁸ the calibration phantom method has an advantage, which is demonstrated as follows. Although the simplest approach was creating a linear regression equation between measured HMRs with both LE and ME collimators, the empirical method cannot be applicable to other camera-collimator combinations or multicenter study protocols. The second approach was based on multi-window acquisition methods. However, subtraction of sub-energy window usually shows low counts, which caused errors in calculation.¹⁴ In contrast, the phantom-based method used in this study is considered to be a simple method to understand differences in camera and collimator systems.¹⁰ With this phantom, because of the homogeneous and flat distribution of the tracer, the reproducibility of HMRs was excellent when the acquisition condition was the same. It was also confirmed that in JSNM-working group databases, the HMR measured with LE-type collimators and corrected by the calibration phantom showed similar normal distribution comparable to that from ME collimators.^{10,16}

In 225 experiments of 84 institutions, the similar collimators, for example LEHR and LEGP, did not show the same conversion coefficient, depending on the vendors. Even in the same vendor, the ELEGP collimator made from 2002 to 2004 showed significantly different values compared with that made after 2008, and the latter showed higher HMRs. This sort of modification and improvement of collimator design has been performed in companies, although the name of collimators was the same. According to the results of this study, the collimator types might be classified into 7 or 8 major subgroups. Hence, two types, namely LE and ME types, are considered a rough classification at present, and the borders of LE and ME types are obscure.

Feasibility for converting to the standard HMR was investigated in this study. In the multicenter study for differentiating dementia with Lewy bodies and Alzheimer disease, HMRs derived from LE collimators were converted to institutional ME-type comparable values.¹⁰ In the study, we assumed that the differences among various ME types were small, and combined distribution of HMR was improved after correction. Because we cannot use a specific collimator from one vendor as a single standard, our proposal is to use the average K_{standard} of MEGP collimators as the standard. With this approach, only an initial phantom experiment is required

when a new camera system is installed. Although mathematical values might have been used as the standard, all institutions should change their HMRs for institutional daily practice.

The cross-calibration method can be used to apply other published studies to one's own institution. For example, a published study used the LE collimator, and the LME collimator might be used in an individual hospital. Based on the ADMIRE-HF study showing a threshold of 1.60 for good and poor prognosis in patients with chronic heart failure using a LE-type collimator,¹² the users of the LME collimator can assume that it is comparable to 1.91 in their institution. If the HMR of 1.77 was used to differentiate dementia with Lewy bodies and others using LE-type collimators,¹⁹ a threshold of 1.77 can be translated to 2.16 for users of the LME collimator. Although a number of studies using a certain threshold of HMR are valid in the similar acquisition conditions, we might be able to integrate experiences of published MIBG studies using this sort of cross-calibration.

When a prediction model is considered for predicting future mortality, current large-scale databases might be prepared using the conventional LEHR collimators.²⁰ Recently, HMRs have been gradually increasing because new collimators covering ^{123}I energy have become available in the nuclear medicine field. If an HMR from ME-comparable conditions is directly used for predicting mortality rate, it may underestimate the risk for future events, and the measured HMR should be converted to LE-comparable values.

LIMITATIONS

Even after the standardization based on the phantom study, we found slight underestimation of HMRs in the range of $\text{HMR} > 2.5$, probably due to the structural difference between the phantom and the human body. One of the important differences in human is complicated down-scatter activity from the high-energy photons coming from outside of the field of view, such as liver, kidney, and bladders.

While complete correction from a physical point of view is ideal in a whole range, the major purpose of standardization is its use in determining a threshold for prognosis and a lower normal range. From this consideration, the most important range of HMR was around 1.6-1.7 for discriminating good and bad prognosis, and a threshold of 2.0-2.2 between normal and abnormal.^{2,12,13,16} In other words, the normal or higher range has no prognostic meaning. Finally, standard HMR used averaged values from 44 experiments with the commonest ME types, which may be modified when required.

NEW KNOWLEDGE GAINED

In terms of HMR calculation, the collimator type was classified not simply into two LE and ME types but includes various intermediate types. Using the cross-calibration phantom method, however, institutional HMRs can be converted to standardized HMRs comparable to the commonest ME-collimator. The cross-calibration method works well in the range of low and normal HMRs when classifying into main risk groups.

Acknowledgments

Authors thank physicians and technologists participating in this study. The authors also appreciate the collaborations of Ms. Yumiko Kirihara and Mr. Kouta Aoyagi of FUJIFILM RI Pharma, Co. Ltd. in assisting phantom experiments. This work was partly supported by Grants-in-Aid for Scientific Research in Japan. The authors would like to thank Mr. Ronald Belisle for his editorial assistance of the manuscript.

Conflict of interest

Kenichi Nakajima, MD, PhD has a collaborative research work for developing software with FUJIFILM RI Pharma, Co. Ltd, Tokyo, Japan.

Disclosures

None.

Open Access

This article is distributed under the terms of the Creative Commons Attribution License which permits any use, distribution, and reproduction in any medium, provided the original author(s) and the source are credited.

APPENDIX

Participated institutions included Asahikawa City Hospital (Asahikawa), Bell Land General Hospital (Sakai), Chubu Medical Center Kizawa Memorial Hospital (Minokamo), Chuno Kosei Hospital (Seki), Dokkyo Medical University (Shimotsuga), Fukushima Medical University (Fukushima), Gifu Prefectural General Medical Center (Gifu), Gifu University Hospital (Gifu), Haibara General Hospital (Makinohara), Hakodate Municipal Hospital (Hakodate), Higashiosaka City General Hospital (Higashiosaka), Hiroshima Red Cross Hospital & Atomic-bomb Survivors Hospital (Hiroshima), Iizuka Hospital (Iizuka), Ikeda Municipal Hospital (Ikeda), Itami City Hospital (Itami), Japanese Red Cross Asahikawa Hospital (Asahikawa), Japanese Red Cross Ashikaga Hospital (Ashikaga), Japanese Red Cross Gifu Hospital (Gifu), Japanese Red Cross Kitami

Hospital (Kitami), Japanese Red Cross Kyoto Daini Hospital (Kyoto), Jichi Medical University Hospital (Shimotsuke), Juntendo Tokyo Koto Geriatric Medical Center (Tokyo), Juntendo University Hospital (Tokyo), Juntendo University Nerima Hospital (Tokyo), Juntendo University Urayasu Hospital (Urayasu), Kanagawa Prefectural Ashigarakami Hospital (Ashigarakami-gun), Kanazawa Municipal Hospital (Kanazawa), Kanazawa University Hospital (Kanazawa), Kawasaki Hospital (Kobe), Keio University Hospital (Tokyo), Kin-ikyo Chuo Hospital (Sapporo), Konan Kakogawa Hospital (Kakogawa), Kyoto Prefectural University of Medicine - University Hospital (Kyoto), Mimihara Oimatsu Clinic (Sakai), Murakami Memorial Hospital Asahi University (Gifu), Nagaoka Red Cross Hospital (Nagaoka), Nagasaki Rousai Hospital (Sasebo), Nagoya City East Medical Center (Nagoya), National Center for Geriatrics and Gerontology (Obu), National Center for Global Health and Medicine (Tokyo), National Cerebral and Cardiovascular Center (Suita), National Hospital Organization Disaster Medical Center (Tachikawa), National Hospital Organization Kumamoto Saishunso National Hospital (Koshi), National Hospital Organization Minami Kyoto Hospital (Joyo), National Hospital Organization Okinawa National Hospital (Ginowan), National Hospital Organization Tokyo National Hospital (Kiyose), National Hospital Organization Yokohama Medical Center (Yokohama), National Kyushu Medical Center (Fukuoka), Nippon Medical School Hospital (Tokyo), Nishikobe Medical Center (Kobe), NTT Medical Center Tokyo (Tokyo), Obihiro-Kosei General Hospital (Obihiro), Ogaki Municipal Hospital (Ogaki), Okayama Kyokuto Hospital (Okayama), Okayama University Hospital (Okayama), Osaka General Medical Center (Osaka), Rumoi Municipal Hospital (Rumoi), Saiseikai Kumamoto Hospital (Kumamoto), Saiseikai Noe Hospital (Osaka), Sapporo City General Hospital (Sapporo), Sapporo-Kosei General Hospital (Sapporo), Seihoku Chuo Hospital (Goshogawara), Shizuoka General Hospital (Shizuoka), Showa General Hospital (Kodaira), Sunagawa City Medical Center (Sunagawa), Surugadai Nihon University Hospital (Tokyo), Suzuka Central General Hospital (Suzuka), Tenri Hospital (Tenri), The Cardiovascular Institute Hospital (Tokyo), The Jikei University Hospital (Tokyo), Toho University Omori Hospital (Tokyo), Tohoku University Hospital (Sendai), Tokyo Medical University (Tokyo), Tokyo Medical University Hospital (Hachioji), Tokyo Metropolitan Geriatric Hospital and Institute of Gerontology (Tokyo), Tokyo Women's Medical University Hospital (Tokyo), Toranomom Hospital (Tokyo), Tottori University Hospital (Yonago), Toyonaka Municipal Hospital (Toyonaka), Tsukuba University Hospital (Tsukuba), Yোগogawa Christian Hospital (Osaka), Yokohama City

University Hospital (Yokohama), Yokohama City University Medical Center (Yokohama), and Yokohama Minami Kyousai Hospital (Yokohama).

References

1. Verberne HJ, Brewster LM, Somsen GA, van Eck-Smit BL. Prognostic value of myocardial ¹²³I-metaiodobenzylguanidine (MIBG) parameters in patients with heart failure: A systematic review. *Eur Heart J* 2008;29:1147-59.
2. Kuwabara Y, Tamaki N, Nakata T, Yamashina S, Yamazaki J. Determination of the survival rate in patients with congestive heart failure stratified by ¹²³I-MIBG imaging: A meta-analysis from the studies performed in Japan. *Ann Nucl Med* 2011;25:101-7.
3. Tamaki N. Guidelines for clinical use of cardiac nuclear medicine (JCS 2005). *Circ J* 2005;69:1125-202 (Revision on the web site 2010).
4. Estorch M, Camacho V, Paredes P, Rivera E, Rodriguez-Revelto A, Flotats A, et al. Cardiac ¹²³I-metaiodobenzylguanidine imaging allows early identification of dementia with Lewy bodies during life. *Eur J Nucl Med Mol Imaging* 2008;35:1636-41.
5. Nakajima K, Yoshita M, Matsuo S, Taki J, Kinuya S. Iodine-123-MIBG sympathetic imaging in Lewy-body diseases and related movement disorders. *Q J Nucl Med Mol Imaging* 2008;52:378-87.
6. Merlet P, Benvenuti C, Moyse D, Pouillart F, Dubois-Rande JL, Duval AM, et al. Prognostic value of MIBG imaging in idiopathic dilated cardiomyopathy. *J Nucl Med* 1999;40:917-23.
7. Veltman CE, Boogers MJ, Meinardi JE, Al Younis I, Dibbets-Schneider P, Van der Wall EE, et al. Reproducibility of planar (123I)-meta-iodobenzylguanidine (MIBG) myocardial scintigraphy in patients with heart failure. *Eur J Nucl Med Mol Imaging* 2012;39:1599-608.
8. Flotats A, Carrio I, Agostini D, Le Guludec D, Marcassa C, Schafers M, et al. Proposal for standardization of ¹²³I-metaiodobenzylguanidine (MIBG) cardiac sympathetic imaging by the EANM Cardiovascular Committee and the European Council of Nuclear Cardiology. *Eur J Nucl Med Mol Imaging* 2010;37:1802-12.
9. Nakajima K, Matsubara K, Ishikawa T, Motomura N, Maeda R, Akhter N, et al. Correction of iodine-123-labeled meta-iodobenzylguanidine uptake with multi-window methods for standardization of the heart-to-mediastinum ratio. *J Nucl Cardiol* 2007;14:843-51.
10. Nakajima K, Okuda K, Matsuo S, Yoshita M, Taki J, Yamada M, et al. Standardization of metaiodobenzylguanidine heart to mediastinum ratio using a calibration phantom: Effects of correction on normal databases and a multicentre study. *Eur J Nucl Med Mol Imaging* 2012;39:113-9.
11. Okuda K, Nakajima K, Hosoya T, Ishikawa T, Konishi T, Matsubara K, et al. Semi-automated algorithm for calculating heart-to-mediastinum ratio in cardiac Iodine-123 MIBG imaging. *J Nucl Cardiol* 2011;18:82-9.
12. Jacobson AF, Senior R, Cerqueira MD, Wong ND, Thomas GS, Lopez VA, et al. Myocardial iodine-123 meta-iodobenzylguanidine imaging and cardiac events in heart failure. Results of the prospective ADMIRE-HF (AdreView Myocardial Imaging for Risk Evaluation in Heart Failure) study. *J Am Coll Cardiol* 2010;55:2212-21.
13. Nakata T, Nakajima K, Yamashina S, Yamada T, Momose M, Kasama S, et al. A pooled analysis of multicenter cohort studies of ¹²³I-MIBG imaging of sympathetic innervation for assessment of long-term prognosis in heart failure. *JACC Cardiovasc Imaging* 2013;6:772-84.
14. Verberne HJ, Feenstra C, de Jong WM, Somsen GA, van Eck-Smit BL, Busemann Sokole E. Influence of collimator choice and simulated clinical conditions on ¹²³I-MIBG heart/mediastinum ratios: A phantom study. *Eur J Nucl Med Mol Imaging* 2005;32:1100-7.
15. Inoue Y, Suzuki A, Shirouzu I, Machida T, Yoshizawa Y, Akita F, et al. Effect of collimator choice on quantitative assessment of cardiac iodine 123 MIBG uptake. *J Nucl Cardiol* 2003;10:623-32.
16. Nakajima K. Normal values for nuclear cardiology: Japanese databases for myocardial perfusion, fatty acid and sympathetic imaging and left ventricular function. *Ann Nucl Med* 2010;24:125-35.
17. Chen J, Garcia EV, Galt JR, Folks RD, Carrio I. Improved quantification in ¹²³I cardiac SPECT imaging with deconvolution of septal penetration. *Nucl Med Commun* 2006;27:551-8.
18. Inoue Y, Abe Y, Itoh Y, Asano Y, Kikuchi K, Sakamoto Y, et al. Acquisition protocols and correction methods for estimation of the heart-to-mediastinum ratio in ¹²³I-metaiodobenzylguanidine cardiac sympathetic imaging. *J Nucl Med* 2013;54:707-13.
19. King AE, Mintz J, Royall DR. Meta-analysis of ¹²³I-MIBG cardiac scintigraphy for the diagnosis of Lewy body-related disorders. *Mov Disord* 2011;26:1218-24.
20. Nakajima K, Nakata T, Yamada T, Yamashina S, Momose M, Kasama S, et al. A prediction model for 5-year cardiac mortality in patients with chronic heart failure using I-123 meta-iodobenzylguanidine imaging. *Eur J Nucl Med Mol Imaging* 2014. doi: 10.1007/s00259-014-2759-x.